Low-cost tightly coupled GPS/INS integration based on a nonlinear Kalman filtering design

Yong Li, Jinling Wang, Chris Rizos, Peter Mumford, and Weidong Ding
University of New South Wales

BIOGRAPHY

Yong Li is a Research Fellow at the School of Surveying & Spatial Information Systems, the University of New South Wales (UNSW). Yong obtained a Doctor of Philosophy in flight dynamics in 1997. From 2000 to 2002 he was a STA Fellow at the Japanese Aerospace Exploration Agency (JAXA, formerly the National Aerospace Laboratory). Yong worked at the Beijing Institute of Control Engineering for GPS space applications from 1997 to 2000. His current research interests include integration of GPS and INS, GPS receiver architectures, GPS-based attitude determination, and optimal estimation/filtering theory and applications.

Jinling Wang is a senior lecturer in the School of Surveying & Spatial Information System at the UNSW. Jinling is a member of the Editorial Board for the international journal GPS Solutions, and Chairman of the study group on pseudolite applications in positioning and navigation within the International Association of Geodesy's Commission 4. He was 2004 President of the International Association of Chinese Professionals in Global Positioning Systems (CPGPS). Jinling holds a PhD in GPS/Geodesy from Curtin University of Technology, Australia.

Chris Rizos is a graduate of UNSW; obtaining a Bachelor of Surveying in 1975, and a Doctor of Philosophy in 1980 in Satellite Geodesy. Chris is currently the Head of the School of Surveying and Spatial Information Systems at UNSW. He has been researching the technology and high precision applications of GPS since 1985, and has published over 200 papers, as well as having authored and co-authored several books relating to GPS and positioning technologies. Chris is a Fellow of the International Association of Geodesy (IAG), Chair of the IAG's Commission 4 "Positioning and Applications", member of the Executive of the U.S. Institute of Navigation's Satellite Division, a member of the Governing Board of the International GNSS Service, and a member of the Australian GNSS Coordination Committee.

Peter Mumford is a Research Assistant in the Satellite Navigation and Positioning laboratory, at the School of Surveying & Spatial Information Systems, UNSW, Sydney Australia. Currently he is working on GNSS receiver design and INS/GNSS integration. Peter has an Engineering degree in Surveying, and a Science degree in Mathematics. His interests are in FPGA design, software, RF and electronic design.

Weidong Ding is currently a Ph.D. student in the School of Surveying & Spatial Information Systems, UNSW. Weidong received his B.E. in Electrical Engineering from Beijing Polytechnic University, China, and his M.E in Electrical Engineering from the UNSW. His research is focused on developing an integrated positioning and geo-referencing platform for kinematic positioning that addresses mobile mapping applications.

ABSTRACT

This paper describes the design of a tightly coupled GPS/INS integration system based on nonlinear Kalman filtering methods. The traditional methods include linearization of the system around a nominal trajectory, and the extended Kalman filtering (EKF) method which linearizes the system around the previous estimate, or the predication, whichever is available. The recently proposed sigma-point Kalman filtering (SPKF) method uses a set of weighted samples (sigma points) to completely capture the first and second order moments of the prior random variable. In contrast to the EKF, the SPKF has a simpler implementation as it does not require the Jacobian matrices – the computation of which may lead to analytical or computational problems in some applications.

This research is conducted under the Australian Cooperative Research Centre (CRC) for Spatial Information (CRC-SI) project 1.3 "Integrated Positioning and Geo-referencing Platform". The project aims to develop a generic hardware/software platform for positioning and imaging sensor integration. The current work focuses on development of software and algorithms,

and a field programmable gate arrays (FPGA) based GPS/INS data logging system.

In the current development phase, a tightly coupled GPS/INS integration system based on a linearization around the INS solution has been designed and implemented. The system uses the GPS pseudorange and Doppler measurements to estimate the INS errors. This paper describes further developments of the integration filter design based on the EKF and SPKF methodologies, in order to compare the performance of nonlinear filtering approaches. Experimental results are presented and further planned developments are outlined.

INTRODUCTION

The integration of GPS and INS can overcome the defects of INS or GPS standalone systems, and benefits from the complementary characteristics of the two systems. To achieve the highest accuracy, multiple dual-frequency GPS receivers can be used in the integrated system to derive accurate baseline solutions from the carrier phase measurements [1]. However, there are many applications requiring a low-cost medium-precision integration system based on a low-cost GPS receiver and IMU, as for example the guidance and navigation of unmanned vehicles [2]. In the design of such a system, a tightly coupled integration approach is more sophisticated than the loosely coupled one [3]. For example, tight integration uses the GPS pseudorange/Doppler measurements directly, and the INS errors can be continuously corrected even if the number of visible GPS satellites drops to below four. On the other hand, a tightly coupled integration algorithm introduces more nonlinear properties into the system. For instance, a loosely coupled system isolates the nonlinear GPS range/range-rate equations to the GPS navigation calculation module. However, nonlinear terms arising from tight integration need to be carefully considered in the design of the integration Kalman filter. The nonlinear issues usually arise from the range and range-rate measurement equations, the discretization of the INS error model, and the triangular terms associated with the attitude angles. The nonlinear property associated with the attitude matrix also affects the lever arm term if the lever arm is expressed in the body frame system.

Most state-of-the-art GPS/INS integration systems are designed to estimate the INS solution errors using the GPS measurement data. The INS error propagation equation is the system equation in the integrated systems. In tightly coupled GPS/INS integration, the GPS range and range-rate data are utilized and the range and range-rate measurement equations are linearized around the INS solution. The standard Kalman filter is then applied to estimate the INS errors. This scheme has been demonstrated by many successful systems and their applications over the past two decades [3][4]. Recently application of nonlinear filtering methods to integrated navigation has been investigated in the literature [2][5]. In these investigations the differential equation of the INS mechanization or the kinematical equations of the host platform is chosen as the system dynamics model. This design unavoidably introduces nonlinearities to the filtering system even in a loosely coupled GPS/INS integration system where the GPS position/velocity solution is directly applied.

The extended Kalman filter is the “standard” approach for state estimation of nonlinear systems over the past three decades [6]. The principal idea of the EKF is linearization of the system equation and/or the measurement equation around the previous estimate or the current prediction. The linearized system is then represented by the Jacobians of the nonlinear system/measurement functions. The normal Kalman filtering formulae are applied to the linearized system. The procedure produces the sub-optimal estimate of the state of the system. The EKF has some defects, such as difficulty in implementation, difficult to tune, and the first order term is insufficiently accurate to approximate the nonlinearities of the system [7].

The sigma-point Kalman filter was developed to overcome the limitation of the EKF. Distinguishing itself from the normal Kalman filter, the SPKF calculates the filtering parameters by utilization of a set of sampling-like points, the so-called the “sigma points” - which can be mapped into the state space or the measurement space through the nonlinear functions of the system directly, instead of linearization through the Jacobians. The parameters derived from the sigma points include the SPKF gain matrix, the state prediction and its covariance, the measurement prediction and its covariance, as well as the estimate covariance [7-9]. However, the EKF calculates the covariance matrices and the Kalman filtering gain matrix using the Jacobians. The EKF is the first order approximation of the nonlinear system and thus may introduce larger errors to the solution, especially if the system has large nonlinearities and the higher order terms are neglected. The SPKF approach is expected to give a better approximation to the nonlinear system because it is easier to approximate a probability distribution than it is to approximate an arbitrary nonlinear function or transformation [7].

This paper develops a tightly coupled GPS/INS integrated system using the SPKF approach. The research is conducted under the CRC for Spatial Information (CRC-SI) project 1.3 “Integrated Positioning and Geo-referencing Platform”. The aims of the project include: (1) to develop a generic integrated positioning/geo-referencing platform system based on FPGA technology, that can be subsequently reconfigured for optimized

positioning and spatial data acquisition applications; and (2) to develop a suite of software that allows for precise, time-synchronized measurement logging, sensor control, real-time data processing, and sundry operations necessary to support such mapping applications.

OPTIMAL ESTIMATION FOR NONLINEAR SYSTEMS

Consider the nonlinear discrete-time system below

$$\mathbf{x}(k+1) = \mathbf{f}[\mathbf{x}(k), k] + \mathbf{G}(k+1, k)\mathbf{w}(k) \quad (1)$$

$$\mathbf{z}(k+1) = \mathbf{h}[\mathbf{x}(k+1), k+1] + \mathbf{v}(k+1) \quad (2)$$

where $\mathbf{x}(k)$ is the state of the system at k, and $\mathbf{z}(k)$ is the measurement vector. The vectors $\mathbf{w}(k)$ and $\mathbf{v}(k)$ are the system noise and measurement noise respectively.

Extended Kalman Filter

The EKF applies the Kalman filter to nonlinear systems by simply linearizing all the nonlinear models so that the traditional linear Kalman filter equations can be applied. The extended Kalman filter (EKF) gives the estimate and the covariance [6]

$$\hat{\mathbf{x}}(k+1|k+1) = \hat{\mathbf{x}}(k+1|k) + \mathbf{K}(k+1)[\mathbf{z}(k+1) - \hat{\mathbf{z}}(k+1|k)] \quad (3)$$

$$\mathbf{P}(k+1|k+1) = [\mathbf{I} - \mathbf{K}(k+1)\mathbf{H}(k+1)]\mathbf{P}(k+1|k) \quad (4)$$

The prediction of the state and its covariance are

$$\hat{\mathbf{x}}(k+1|k) = \mathbf{f}[\hat{\mathbf{x}}(k|k), k] \quad (5)$$

$$\mathbf{P}(k+1|k) = \mathbf{F}(k+1, k)\mathbf{P}(k|k)\mathbf{F}^{\mathrm{T}}(k+1, k) + \mathbf{G}(k+1, k)\mathbf{Q}(k)\mathbf{G}^{\mathrm{T}}(k+1, k) \quad (6)$$

The prediction of measurement is

$$\hat{\mathbf{z}}(k+1|k) = \mathbf{h}[\hat{\mathbf{x}}(k+1|k), k+1] \quad (7)$$

The Kalman gain matrix is

$$\mathbf{K}(k+1) = \mathbf{P}(k+1|k)\mathbf{H}^{\mathrm{T}}(k+1) \cdot [\mathbf{H}(k+1)\mathbf{P}(k+1|k)\mathbf{H}^{\mathrm{T}}(k+1) + \mathbf{R}(k+1)]^{-1} \quad (8)$$

where $\mathbf{F}(k+1,k)$ and $\mathbf{H}(k+1)$ are Jacobian matrices associated with $\mathbf{f}$ and $\mathbf{h}$

$$\mathbf{F}(k+1, k) = \frac{\partial}{\partial \mathbf{x}}\mathbf{f}[\hat{\mathbf{x}}(k|k), k] \quad (9)$$

$$\mathbf{H}(k+1) = \frac{\partial}{\partial \mathbf{x}}\mathbf{h}[\hat{\mathbf{x}}(k+1|k), k+1] \quad (10)$$

Sigma Point Kalman Filter

The sigma point Kalman filter, according to [7-9], can be summarized as follows. The sigma point Kalman filter updates the predication after the measurements arrive:

$$\hat{\mathbf{x}}(k+1|k+1) = \hat{\mathbf{x}}(k+1|k) + \mathbf{S}(k+1)[\mathbf{z}(k+1) - \hat{\mathbf{z}}(k+1|k)] \quad (11)$$

Comparing Eq. (11) with Eq. (3), one can find that the sigma point filter has the same prediction-correction structure as the normal Kalman filter. The gain matrix **S** in Eq. (11) can be referred to as the SPKF gain matrix, in a similar way to the Kalman filter's gain matrix **K** in Eq. (3). The estimate covariance is

$$\mathbf{P}(k+1|k+1) = \mathbf{P}(k+1|k) - \mathbf{S}(k+1) \cdot [\mathbf{R}(k+1) + \mathbf{P}_{zz}(k+1|k+1)]\mathbf{S}^{\mathrm{T}}(k+1) \quad (12)$$

The SPKF gain matrix **S** is

$$\mathbf{S}(k+1) = \mathbf{P}_{xz}(k+1|k)[\mathbf{R}(k+1) + \mathbf{P}_{zz}(k+1|k+1)]^{-1} \quad (13)$$

The SPKF calculates the first and second moments of the priori random variables by utilization of the sigma points. As opposed to the particle filtering methodologies, the sigma points are deterministically calculated from the current estimate of its covariance. The sigma points can be mapped into the state space or the measurement space through the nonlinear functions of the system. The projection is then used for calculation of the filtering parameters. The Jacobians are thus no longer needed. Fig. 1 illustrates the mapping of the SPKF versus that of the EKF, through the transformation of the nonlinear function **f** and its Jacobian **F** respectively. The dot-line ellipse represents the true covariance. The solid-line ellipse represents the calculated covariance. The SPKF approach estimates are expected to be closer to the true values than using the EKF approach.

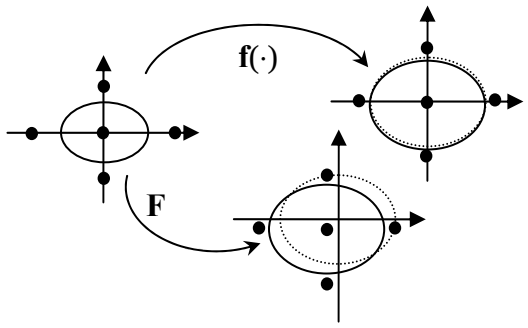

Fig 1. Illustration of projections of SPKF and EKF

For a system described by an n-dimension state, the 2n+1 sigma points will be used. The reduced sigma point filtering method can be found in [10]. Hereafter the

normal 2n+1 sigma points will be used. The sigma points in the state space and associated weights are:

$$\mathbf{X}_0(k|k) = \hat{\mathbf{x}}(k|k), \quad W_0 = \kappa/\{n+\kappa\} \tag{14}$$

$$\mathbf{X}_i(k|k) = \hat{\mathbf{x}}(k|k) + \sqrt{(n+\kappa)\mathbf{P}(k|k)}, \; W_i = 0.5/(n+\kappa) \tag{15}$$

$$\mathbf{X}_{i+n}(k|k) = \hat{\mathbf{x}}(k|k) - \sqrt{(n+\kappa)\mathbf{P}(k|k)}, \; W_{i+n} = 0.5/(n+\kappa) \tag{16}$$

The sigma points of predication are then

$$\mathbf{X}_i(k+1|k) = \mathbf{f}[\mathbf{X}_i(k|k), k] \tag{17}$$

The predication and its covariance are

$$\hat{\mathbf{x}}(k+1|k) = \sum_{i=0}^{2n} W_i \mathbf{X}_i(k+1|k) \tag{18}$$

$$\mathbf{P}(k+1|k) = \sum_{i=0}^{2n} W_i [\mathbf{X}_i(k+1|k) - \hat{\mathbf{x}}(k+1|k)] \cdot [\mathbf{X}_i(k+1|k) - \hat{\mathbf{x}}(k+1|k)]^T \tag{19}$$

The sigma points of measurements are

$$\mathbf{Z}_i(k+1|k) = \mathbf{h}[\mathbf{X}_i(k+1|k), k+1] \tag{20}$$

The predication of measurements and its covariance are

$$\hat{\mathbf{z}}(k+1|k) = \sum_{i=0}^{2n} W_i \mathbf{Z}_i(k+1|k) \tag{21}$$

$$\mathbf{P}_{zz}(k+1|k) = \sum_{i=0}^{2n} W_i [\mathbf{Z}_i(k+1|k) - \hat{\mathbf{z}}(k+1|k)] \cdot [\mathbf{Z}_i(k+1|k) - \hat{\mathbf{z}}(k+1|k)]^T \tag{22}$$

$$\mathbf{P}_{xz}(k+1|k) = \sum_{i=0}^{2n} W_i [\mathbf{X}_i(k+1|k) - \hat{\mathbf{x}}(k+1|k)] \cdot [\mathbf{Z}_i(k+1|k) - \hat{\mathbf{z}}(k+1|k)]^T \tag{23}$$

SYSTEM DESCRIPTION

The hardware components of the system include the BEI's Digital Quartz IMU-Navigation Processor (DQI-NP) and the Rockwell's MicroTracker LP GPS receiver. The DQI-NP has two interfaces for communication with external devices. The MicroTracker LP GPS receiver has a 9-pin interface to communicate with the DQI-NP; providing the DQI-NP with the 1PPS for time synchronization and the necessary measurements. For our purpose the DQI-NP is set to operate in the INS-only mode. The GPS raw measurements are logged to a PC through an additional RS232 port. All GPS data are converted to the RINEX format. The hardware configuration and connections are shown in Fig. 2.

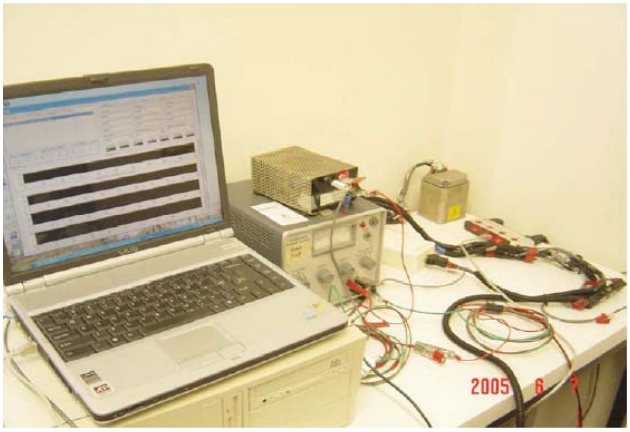

Fig. 2 Hardware components of the integrated GPS/INS system

DQI-NP is a guidance, navigation & control (GN&C) product that uses the BEI Systron Donner Inertial Division's solid-state DQI technology [11]. It is designed around an Inertial Sensor Assembly (ISA) and provides all the basic IMU outputs including delta velocity (ΔV), delta angular vector ($\Delta\theta$). The ISA consists of six single-axis sensors, three Quartz Rate Sensors, three Vibrating Quartz Accelerometers, the drive electronics, preamplifier circuitry for the sensor outputs, and the digital conversion electronics. The main specifications of DQI are listed in Table 1.

Table 1. System specifications of DQI [12]

	Gyro (1σ)	Accelerometer (1σ)
Bias repeatability	10 deg/hr	1.5 mg
In-run stability	3 deg/hr	200 μg
Scale factor	350 ppm	350 ppm
Random walk	0.035 deg/sqrt(hr)	200 μg/sqrt(Hz)
Non-orthogonality	0.5 mrad	0.5 mrad

DESIGN OF INTEGRATED KALMAN FILTER

As the core of the integrated system the Kalman filter must be carefully designed. Because the tightly coupled GPS/INS integration is a nonlinear system, three filtering schemes are adopted in our system: (1) the linearization around the INS solution (hereafter referred to as the linearization method), (2) the EKF, and (3) the SPKF. Both the linearization method and the EKF designs linearize the system around an approximate point, the system state vector, whose components are usually chosen as the INS solution errors and the IMU sensor errors [1,3,4,11,12]. The SPKF does not need to linearize the system, and the nonlinear functions of the system are directly used in the algorithm for producing the sigma

points. Therefore the SPKF-based design can choose the navigation state rather than the error state as the system state of the filter [2][5]. This paper, however, uses the INS error state and the sensor errors as the system state. Thus the three design schemes use the same system state vector. The 15 states of the filter are given in Table 2. The IMU sensor errors are the sum of all sensor errors such as the scale factor error, the bias and the noise.

Table 2. The integration Kalman filter's state definition

State	Definition	Coordinate system
1-3	Position error	NED
4-6	Velocity error	NED
7-9	Attitude error	NED
10-12	Accelerometer error	b-frame
13-15	Gyro error	b-frame

The INS error equation is expressed in the psi-angle error mode[13]:

$$\delta\dot{\mathbf{r}} = -\omega_{en} \times \delta\mathbf{r} + \delta\mathbf{v} \tag{24}$$

$$\delta\dot{\mathbf{v}} = -(\omega_{ie} + \omega_{in}) \times \delta\mathbf{v} - \mathbf{f} \times \delta\psi + \boldsymbol{\varepsilon}_a \tag{25}$$

$$\delta\dot{\psi} = -\omega_{in} \times \delta\psi + \boldsymbol{\varepsilon}_g \tag{26}$$

The sensor errors are modeled as random walk processes

$$\dot{\boldsymbol{\varepsilon}}_a = \mathrm{w}_a \tag{27}$$

$$\dot{\boldsymbol{\varepsilon}}_g = \mathrm{w}_g \tag{28}$$

where $\delta\mathbf{r}$, $\delta\mathbf{v}$, and $\delta\psi$ are the error vectors of position, velocity and angle respectively. ε_a and ε_g are errors of the accelerometers and gyroscopes respectively. w_a and w_g are the white noises associated with accelerometers and gyroscopes respectively

Supposing there are n visible satellites, the measurement equation for satellite #i can be written in following form.

For the method linearizing around the INS solution:

$$\mathrm{z}^{\mathrm{i}} = \frac{(\mathbf{r}^{\mathrm{i}}_{\mathrm{sat}} - \mathbf{r}_{\mathrm{ins}})^{\mathrm{T}}}{\left\|\mathbf{r}^{\mathrm{i}}_{\mathrm{sat}} - \mathbf{r}_{\mathrm{ins}}\right\|}\delta\mathbf{r} + \xi^{\mathrm{i}} \tag{29}$$

$$\dot{\mathrm{z}}^{\mathrm{i}} = \frac{(\mathbf{v}^{\mathrm{i}}_{\mathrm{sat}} - \mathbf{v}_{\mathrm{ins}})^{\mathrm{T}}}{\left\|\mathbf{r}^{\mathrm{i}}_{\mathrm{sat}} - \mathbf{r}_{\mathrm{ins}}\right\|}\delta\mathbf{r} + \frac{(\mathbf{r}^{\mathrm{i}}_{\mathrm{sat}} - \mathbf{r}_{\mathrm{ins}})^{\mathrm{T}}}{\left\|\mathbf{r}^{\mathrm{i}}_{\mathrm{sat}} - \mathbf{r}_{\mathrm{ins}}\right\|}\delta\mathbf{v} + \dot{\xi}^{\mathrm{i}} \tag{30}$$

where z^i and $\dot{z}^i$ are the range and range-rate differences between GPS and INS respectively.

For the EKF:

$$y^i = \frac{(\mathbf{r}^i_{sat} - \mathbf{r}_{ins} + \delta\hat{\mathbf{r}}_{k|k-1})^T}{\left\|\mathbf{r}^i_{sat} - \mathbf{r}_{ins} + \delta\hat{\mathbf{r}}_{k|k-1}\right\|}\delta\mathbf{r} + \xi^i \tag{31}$$

$$\begin{aligned}\dot{y}^i = &\frac{(\mathbf{v}^i_{sat} - \mathbf{v}_{ins} + \delta\hat{\mathbf{v}}_{k|k-1})^T}{\left\|\mathbf{r}^i_{sat} - \mathbf{r}_{ins} + \delta\hat{\mathbf{r}}_{k|k-1}\right\|}\delta\mathbf{r} \\ &+ \frac{(\mathbf{r}^i_{sat} - \mathbf{r}_{ins} + \delta\hat{\mathbf{r}}_{k|k-1})^T}{\left\|\mathbf{r}^i_{sat} - \mathbf{r}_{ins} + \delta\hat{\mathbf{r}}_{k|k-1}\right\|}\delta\mathbf{v} + \dot{\xi}^i\end{aligned} \tag{32}$$

where y^i and $\dot{y}^i$ are the equivalent measurements after the linearization.

For the SPKF:

$$\rho^{\mathrm{i}} = \left\|\mathbf{r}^{\mathrm{i}}_{\mathrm{sat}} - \mathbf{r}_{\mathrm{ins}} + \delta\mathbf{r}\right\| + \xi^{\mathrm{i}} \tag{33}$$

$$\dot{\rho}^{\mathrm{i}} = \frac{(\mathbf{r}^{\mathrm{i}}_{\mathrm{sat}} - \mathbf{r}_{\mathrm{ins}} + \delta\mathbf{r})^{\mathrm{T}}(\mathbf{v}^{\mathrm{i}}_{\mathrm{sat}} - \mathbf{v}_{\mathrm{ins}} + \delta\mathbf{v})}{\left\|\mathbf{r}^{\mathrm{i}}_{\mathrm{sat}} - \mathbf{r}_{\mathrm{ins}} + \delta\mathbf{r}\right\|} + \dot{\xi}^{\mathrm{i}} \tag{34}$$

where ρ^i and $\dot{\rho}^i$ are the range and range-rate measurements.

Low-cost GPS receivers use inexpensive crystal oscillators that drift and introduce clock biases in the pseudorange and frequency shift in the Doppler measurements. These clock terms are common errors in measurements from satellites, and single-differences between satellites can remove them. In this implementation, the between-satellite difference operation is applied to the measurements in order to remove these errors.

The GPS receiver provides orbital data for calculating the position and velocity values for the GPS satellites. It also makes the pseudorange and Doppler measurements. The DQI-NP operates in the INS-only mode and provides the host platform's navigational data, including position in LLA form (latitude, longitude, and altitude), velocity in ENU (east-north-up) form, and the attitude angles. Inside the software all navigational solutions, either from GPS or INS, are transformed to the NED (north-east-down) coordinate system.

The software is implemented in C++ code. Because GPS and INS data are read in parallel, a mechanism for aligning the two data streams is necessary. For instance, the first time-tags of GPS and INS data can be read after initialization. The time-tags can be compared to decide which type of data will be read in the next cycle. If the GPS time-tag is earlier than the INS time-tag, for example at the present reading cycle, the next cycle must read INS data until the INS data 'catches up' with the GPS data.

Conversely, if the GPS data is following the INS data, the next cycle must read GPS data until the GPS 'catches up' with the INS data. Once the difference between the GPS and INS time-tags falls to a small value, the two data can be regarded as being "aligned". The Kalman filter algorithm will then be triggered.

EXPERIMENTS

Static tests

Static tests have been performed in order to evaluate the system. As the SPKF is of most interest, its performance is highlighted. The typical setup of the devices for the static tests is a GPS antenna fixed on the roof of the EE building, at the Kensington Campus of the University of New South Wales. Through a coaxial cable the GPS signal is fed into the room where the GPS receiver and the DQI-NP are located. There is a distance of several metres between the GPS antenna and the INS. This can be treated as the lever arm. As the INS errors are estimated using the GPS data, the corrected INS solution always follows the GPS solution. This phenomenon is reflected in the position curves, e.g. as depicted in Figs 3a and 3b, in which the GPS-only solution (in green lines) is derived from the same data set being used in the integration filter.

To clearly observe the efficiency of the filtering solution tracking the INS error, a forward correction instead of feedback correction is applied to the system. Figure 4a and 4b illustrates the INS-only position (in blue lines) against the GPS/INS integrated solution (in red lines). From Figs 4a and 4b it is evident that the INS errors grow rapidly without the aid of GPS, and the errors can be efficiently compensated for by the GPS through the Kalman filter. The GPS/INS integrated solution (in red lines) is smoother than the GPS-only solution, as shown in Figs 3a and 3b. Therefore the GPS/INS solution is better than a standalone solution either of GPS or INS.

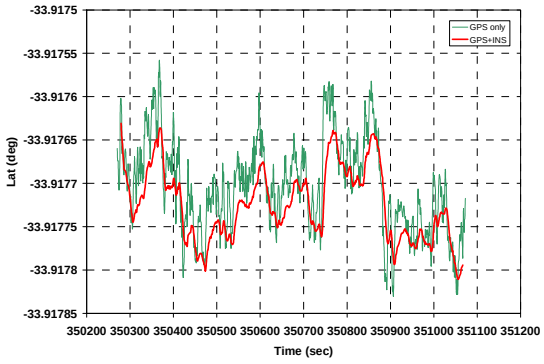

Fig. 3a Latitude solutions, the SPKF vs the GPS-only

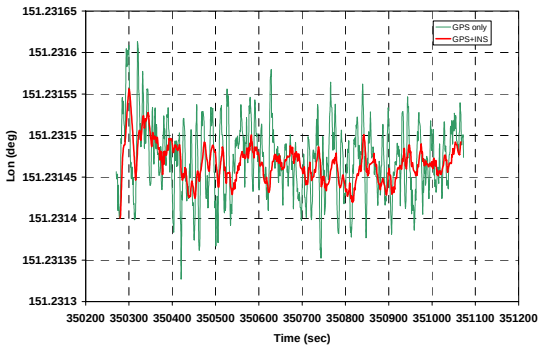

Fig. 3b Longitude solutions, the SPKF vs the GPS-only

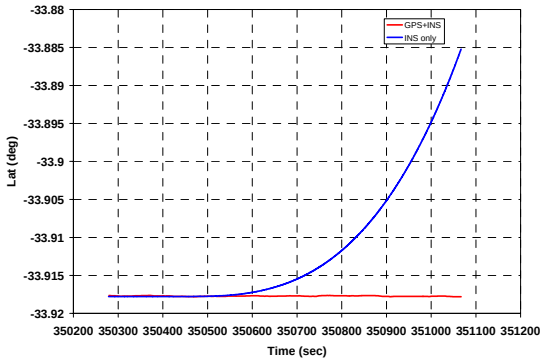

Fig. 4a Latitude solutions, the SPKF vs the INS-only

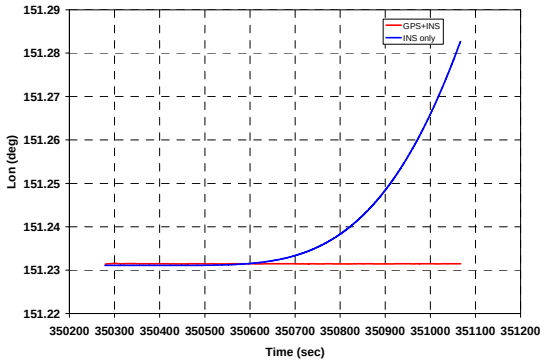

Fig. 4b Longitude solutions, the SPKF vs the INS-only

Three filtering designs give almost the same solution in terms of accuracy. This result agrees with the result in [2] and does not support the "expected" conclusion that the SPKF gives higher solution accuracy. One possible reason is that the nonlinearities of the range and range-rate measurement equations are not large enough and hence the SPKF's better performance is not obvious. This explanation of course would need to be verified by further theoretical analysis. As pointed out in the previous section, the SPKF's biggest advantage over the EKF is that it does not need the Jacobian matrices. This feature makes for more convenient system design, mathematical derivation and software implementation.

Figs 5a and 5b depict the covariance-time curves, the EKF (blue line) against the SPKF (red line). It shows that the SPKF has a fast speed of filter convergence.

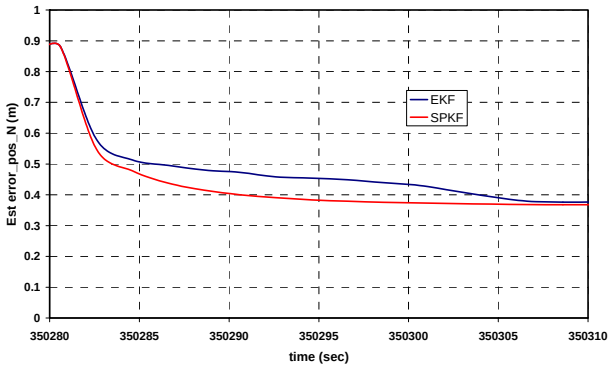

Fig. 5a Covariances in north position, EKF vs SPKF

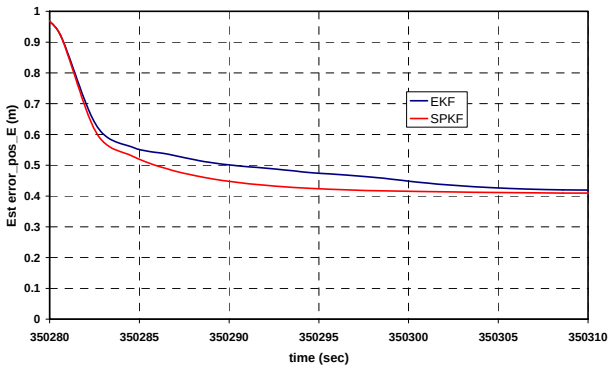

Fig. 5b Covariances in east position, EKF vs SPKF

Kinematic tests

In the kinematic experiments the GPS antennas and the INS were set up on the roof of a car, as shown in Fig. 6. The MicroTracker GPS receiver and a Leica system 530 dual-frequency GPS receiver were used in the tests. The purpose is to determine whether a high quality GPS receiver can improve the performance of the system. The trajectory of the car in the test is plotted in Fig. 7, as derived from the SPKF solution.

Fig. 6 Device installation in the kinematic test

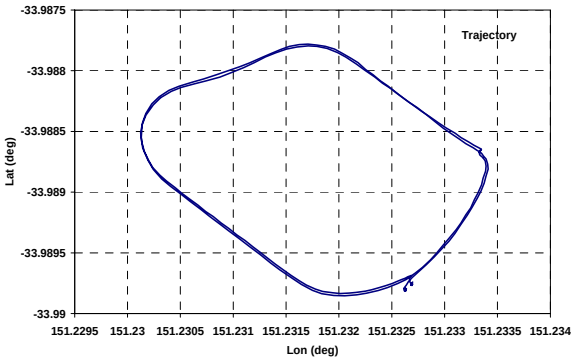

Fig. 7 Trajectory of the car in the kinematic test

The comparison of the GPS-only solution with the GPS/INS integrated solution is depicted in Figs 8a to 8d. It is clear that the GPS/INS integrated solution (in red) is smoother than the GPS-only solution (in green) (8a and 8b). It is particularly obvious when the car is static. In both position and velocity the integrated solution tracks the car's maneuvers very well, as indicated in Figs 8a to 8d. This also demonstrates that the latency caused by the filter is within the allowance for the required accuracy.

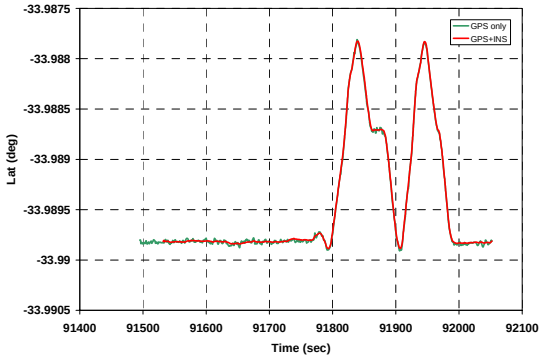

Fig. 8a Latitude solutions, SPKF vs GPS-only

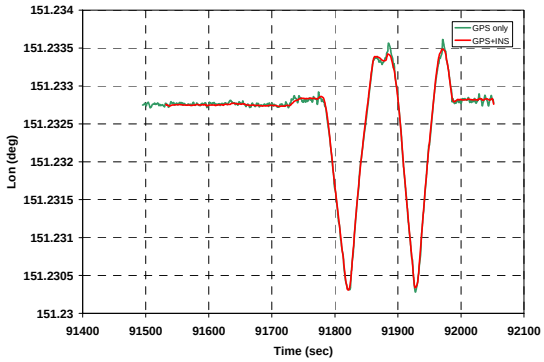

Fig. 8b Longitude solutions, SPKF vs GPS-only

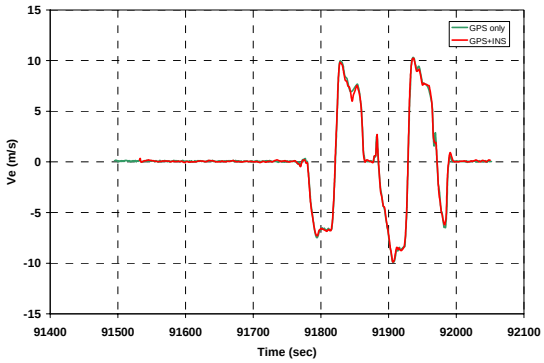

Fig. 8c East velocity solutions, SPKF vs GPS-only

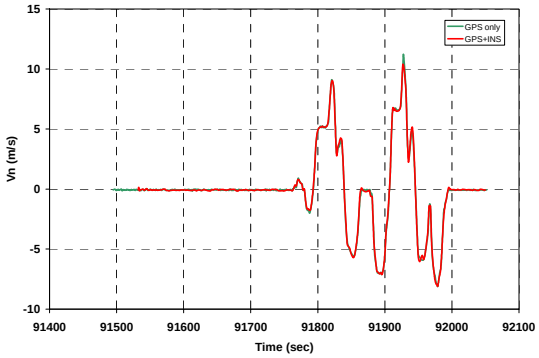

Fig. 8d North velocity solutions, SPKF vs GPS-only

The comparison of the SPKF solution (in red lines) and the INS-only solution (in blue lines) is depicted in Figs 9a to 9d, where the INS drift is obvious. A big discrepancy in initial position is obvious in Figs 9a and 9b. This is caused by the initial error of the INS, a position difference of about 10 km between the test site and the laboratory location. The error is estimated from the GPS data and can be quickly compensated for, as shown in Figs 8a and 8b.

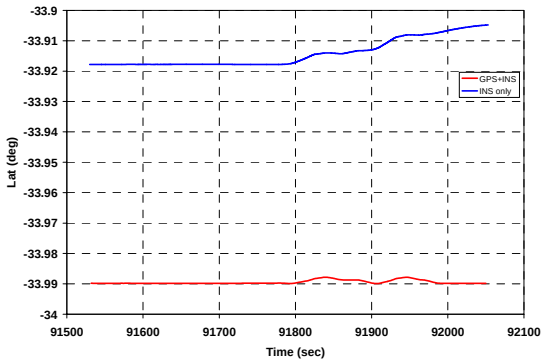

Fig. 9a Latitude solutions, SPKF vs INS-only

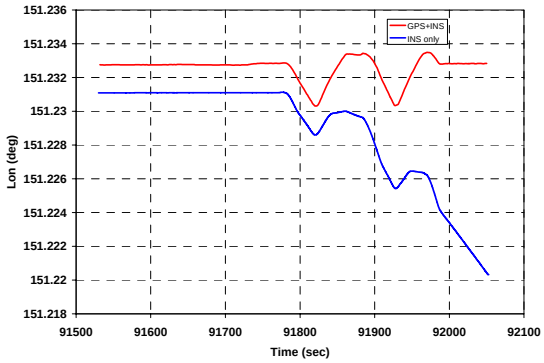

Fig. 9b Longitude solutions, SPKF vs INS-only

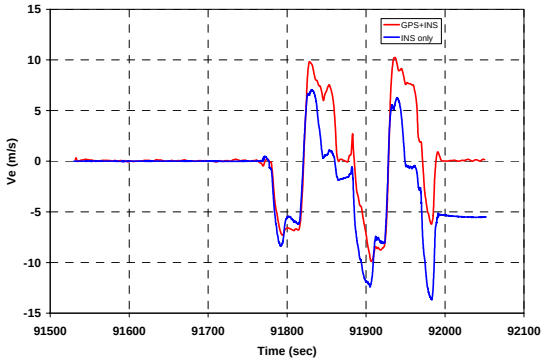

Fig. 9c East velocity solutions, SPKF vs INS-only

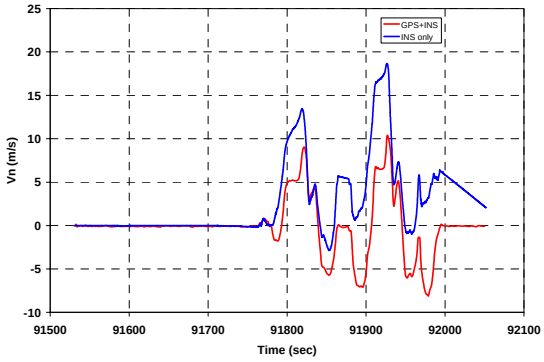

Fig. 9d North velocity solutions, SPKF vs INS-only

The SPKF covariance-time curves in position and velocity are depicted in Figs 10a and 10b respectively. The red lines are the east components and the blue lines are the north components. Comparing the solutions in Figs 8a to 8d, one can find that the biggest changes occur during maneuvers. As the covariance is calculated from the sigma points, it could be influenced by the measurements and the GPS constellation. A further theoretical analysis is needed to verify this.

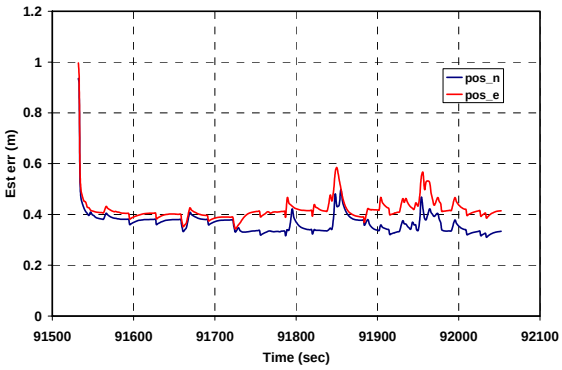

Fig. 10a Position covariance solutions of SPKF

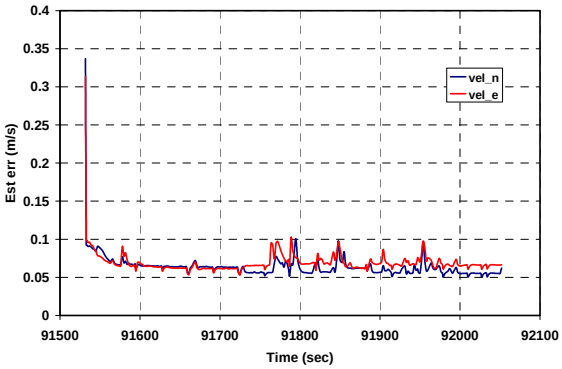

Fig. 10b Velocity covariance solutions of SPKF

CONCLUSIONS

A tightly coupled GPS/INS integration system has been designed and implemented on the basis of nonlinear filtering methods. The new nonlinear filter, the sigma point Kalman filter (SPKF), was compared with traditional methods such as the linearization approach and the extended Kalman filter (EKF). In contrast to the EKF, the SPKF is easier to implement because it does not require the computation of Jacobian matrices. Static and kinematic tests have demonstrated that the SPKF can generate solutions of similar accuracy to those of the EKF. However the SPKF has a faster convergence speed.

Planned further developments include theoretical analysis on the SPKF-based tightly coupled GPS/INS integration system, and migration of the design to the FPGA platform for real-time implementation.

REFERENCES

1. D. A. Grejner-Brzezinska, R. Da, and C. Toth, *GPS Error Modelling and OTF Ambiguity Resolution for High-Accuracy GPS/INS Integrated System*, Journal of Geodesy, Vol.72, 1998, pp. 626-638.
2. R. Van der Merwe, and E. A. Wan, *Sigma-point Kalman Filters for Integrated Navigation*, Proceedings of the 60th Annual Meeting of The Institute of Navigation, Dayton, OH, June 7-9, 2004, pp. 641-654.
3. M. K. Martin and B. C. Detterich, C-MIGITS II Design and Performance, Proceedings of ION GPS-97, Kansas, September 16-19, 1997, pp. 95-102.
4. R. Da, *Investigation of a Low-Cost and High-Accuracy GPS/IMU System*, Proceedings of ION National Technical Meeting 1997, Santa, Monica, California, January 14-16, 1997, pp. 955-963.
5. J. Wendel, J. Metzger, R. Moenikes, A. Maier, G. F. Trommer, *A Performance Comparison of Tightly Coupled GPS/INS Navigation Systems Based onExtended and Sigma Point Kalman Filters*, Proceedings of ION GNSS 2005, Long Beach, CA September 13-16 , 2005, pp. 456-466.
6. C. K. Cui and G. Chen, *Kalman Filtering*, 3rd Ed, Springer, 1999.
7. S. J. Julier and J. K. Uhlmann, *Unscented Filtering and Nonlinear Estimation*, Proceedings of the IEEE, Vol. 92, No. 3, 2004, pp. 401-422.
8. S. Julier, J. Uhlmann, and H. F. Durrant-Whyte, *A New Method for the Nonlinear Transformation of Means and Covariances in Filters and Estimators*, IEEE Trans On AC, Vol. 45, No. 3, 2000, pp. 477-482.
9. T. Lefebvre, H. Bruyninckx, and J. De Schutter, *Comment on "A New Method for the Nonlinear Transformation of Means and Covariances in Filters and Estimators"*, IEEE Trans on AC, Vol. 47, No. 8, 2002, pp. 1406-1408.
10. S. J. Julier and J. K. Uhlmann, *Reduced Sigma Point Filters for the Propagation of Means and Covariances Through Nonlinear Transformations*, http://www.cs.unc.edu/~welch/kalman/media/pdf/ACC02-IEEE1358.pdf, accessed on September 1, 2005.
11. M. K. Martin, and B. C. Detterich, *Digital Quartz IMU - Navigation Processor (DQI-NP) Design and Performance*, Proceedings of ION GPS-97, Kansas, September 16-19, 1997, pp. 161-166.
12. BEI, User's Guide of DQI -- Digital Quartz IMU User's Manual of C-MIGITS II, BEI Systron Donner Inertial Division, California, BEI Technologies Inc., 964008 Rev. A, printed in United States of American, 2002.
13. I. Y. Bar-Itzhack and N. Berman, *Control Theoretical Approach to Inertial Navigation Systems*, Journal of Guidance, Control and Dynamics, Vol. 11, No. 3, 1988, pp. 237-245.